Chinese Chemical Letters 32 (2021) 1220–1223

Contents lists available at ScienceDirect

Chinese Chemical Letters

journal homepage: www.elsevier.com/locate/cclet

Communication

Mitochondrion targeting peptide-modified magnetic graphene oxide delivering mitoxantrone for impairment of tumor mitochondrial functions

Hangqi Zhu[a], Bing Zhang[b,c], Nali Zhu[a], Mingchun Li[a,*], Qilin Yu[a,*]

[a] Key Laboratory of Molecular Microbiology and Technology, Ministry of Education, Department of Microbiology, College of Life Sciences, Nankai University, Tianjin 300071, China
[b] College of Chemistry, State Key Laboratory of Elemento-Organic Chemistry, Nankai University, Tianjin 300071, China
[c] Collaborative Innovation Center of Chemical Science and Engineering (Tianjin), Tianjin 300072, China

ARTICLE INFO

Article history:
Received 25 May 2020
Received in revised form 31 August 2020
Accepted 3 September 2020
Available online 5 September 2020

Keywords:
Magnetic graphene oxide
Nanocarrier
Mitochondrion-targeting peptide
Mitoxantrone
Cancer therapy

ABSTRACT

In this study, we prepared mitochondrion targeting peptide-grafted magnetic graphene oxide (GO) nanocarriers for efficient impairment of the tumor mitochondria. The two-dimensional GOMNP-MitP nanosheets were synthesized by grafting magnetic γ-Fe_2O_3 to the surface of GO, followed by covalent modification of mitochondrion targeting peptide (MitP). GOMNP-MitP exhibited the high capacity of loading the anticancer drug mitoxantrone (MTX), and preferentially targeted the tumor mitochondria. With the aid of alternating magnetic field (AMF), the MTX-loading GOMNP-MitP released MTX to the mitochondria, severely impairing mitochondrial functions, including attenuation of ATP production, decrease in mitochondrial membrane potential (MMP), and further leading to activation of apoptosis. This study realized high-efficient mitochondrion-targeting drug delivery for anticancer therapy by two-dimensional nanoplatforms.

The mitochondria are one of the main organelles in the eukaryotic cells, functioning in energy production, carbohydrate metabolism, and regulation of signal transduction [1,2]. In tumor cells, the mitochondria are closely associated with cell survival in apoptosis-inducing factors, supply of high-level ATPs, and promotion of invasion and metastasis [3,4]. Owing to the great significance to tumor survival and malignant progression of cancers, this organelle is becoming a significant anticancer target to induce mitochondrial dysfunction, followed by energy depletion and apoptosis activation of tumor cells [5,6]. As the development of nanotechnology, some drug-delivery, photodynamic, or photothermal nanoplatforms that target this organelle have been developed to damage it for enhancing the outcome of anticancer therapies [7–10].

Magnetic graphene oxides (GO), *i.e.*, GO grafted by magnetic nanoparticles (*e.g.*, Fe_3O_4 nanoparticles, γ-Fe_2O_3 nanoparticles), are promising two-dimensional nanoplatforms in anticancer therapies [11–14]. These nanoplatforms exhibited good biocompatibility, high photothermal/magnetothermal property, and multifunctionality of magnetic targeting and magnetic resonance imaging [15,16]. In recent years, they have been developed as nanocarriers of anticancer drugs (*e.g.*, doxorubicin, cisplatin, 5-fluorouracil, *etc.*) or photothermal agents to kill tumor cells [17–22]. However, their applications in mitochondrion-targeting anticancer therapies remain to be further investigated.

In this study, we designed a mitochondrion-targeting drug-delivery nanoplatform for cancer therapy, *i.e.*, the mitochondrion-targeting peptide-grafted and magnetic γ-Fe_2O_3 nanoparticle-grafted GO (Scheme 1). Drug-loading and drug-releasing assays was performed to investigate the potential of this nanocomposites as drug carriers using mitoxantrone (MTX), a clinical anticancer drug inducing DNA damage in tumor cells [23]. Confocal microscopy observation and mitochondrion function assays were further performed to explore the mitochondrion-targeting/damaging capacity of the MTX-loading nanocarriers with the aid of alternating magnetic field (AMF).

The initial GO nanosheets were firstly synthesized by the modified Hummer's method [24,25]. To endow the magnetic property of two-dimensional GO nanosheets, $FeCl_3 \cdot 6H_2O$ and hexamethylenetetramine were used to deposit γ-Fe_2O_3 nanoparticles on the surface of GO, obtaining GOMNP [11]. The

* Corresponding authors.
E-mail addresses: nklimingchun@163.com (M. Li), yuqilin@mail.nankai.edu.cn (Q. Yu).

https://doi.org/10.1016/j.cclet.2020.09.003
1001-8417/

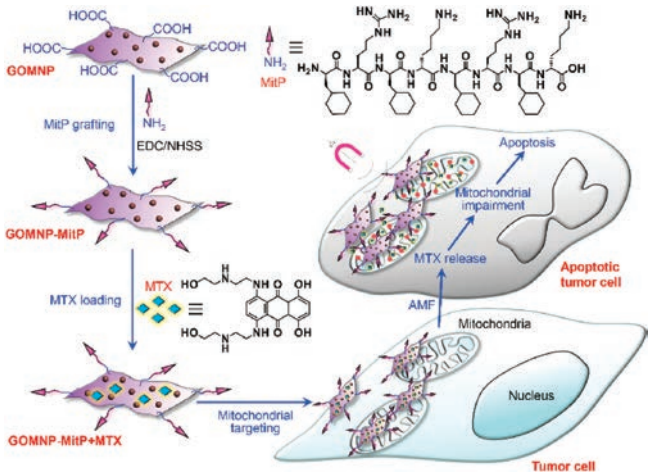

Scheme 1. Illustration of GOMNP-MitP + MTX synthesis for mitochondrion-targeted MTX delivery, mitochondrial impairment and apoptosis induction of tumor cells.

magnetic GO was further grafted by MitP by the EDC/NHS reaction [26], obtaining GOMNP-MitP. SEM observation and EDS mapping analysis showed that both kinds of nanomaterials had abundant nanoparticles on the surfaces, and showed equal distribution of N, S, O, and Fe elements (Figs. 1a and b). As compared to GOMNP that exposed obvious nanoparticles on the surfaces, GOMNP-MitP had a coating layer on the surface of the nanosheets (Fig. 1a). TEM observation further revealed that both GOMNP and GOMNP-MitP had nanosheet morphology, with the nanosheet sizes of 200–400 nm, and with abundant γ-Fe_2O_3 nanoparticles (10–25 nm) on the surface of the nanosheets (Fig. 1c). FT-IR analysis revealed the

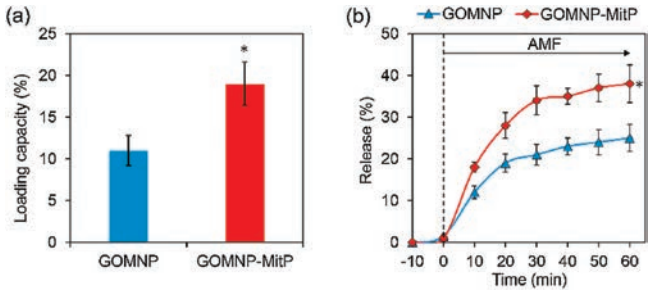

Fig. 2. Loading and AMF-triggered release of MTX by GOMNP and GOMNP-MitP. (a) MTX-loading capacity of the GOs. (b) AMF-triggered release by the GOs. The "0" at the X axis indicates the starting time point of AMF treatment. *indicates significant difference between the groups ($P < 0.05$).

presence of –NH–CO– (1680 nm) and -NH_2 (1340 nm) in GOMNP-MitP, confirming successful MitP grafting on GOMNP (Fig. 1d). Magnetization curves showed that the magnetic GOs had the maximum magnetization value of 50∼55 emu/g, with no obvious hysteresis loop (Fig. 1e), validating their superparamagnetic property. Moreover, under the AMF treatment, both of the GOs exhibited similar temperature curve (from 23 °C to ∼50 °C after 10 min of AMF treatment, Fig. 1f), indicating their excellent AMF-responsive properties.

The drug-loading and drug-releasing capacities of the GO nanocomposites were evaluated by using the important anticancer drug MTX. After 24 h of co-incubation of the GOs with MTX, GOMNP-MitP exhibited higher MTX-loading capacity than GOMNP (19% *versus* 11%, Fig. 2a). This result indicated that MitP grafting might improve the loading capacity of the nanocomposites, which may be attributed to the drug-retaining effect of the peptide on the nanosheets.

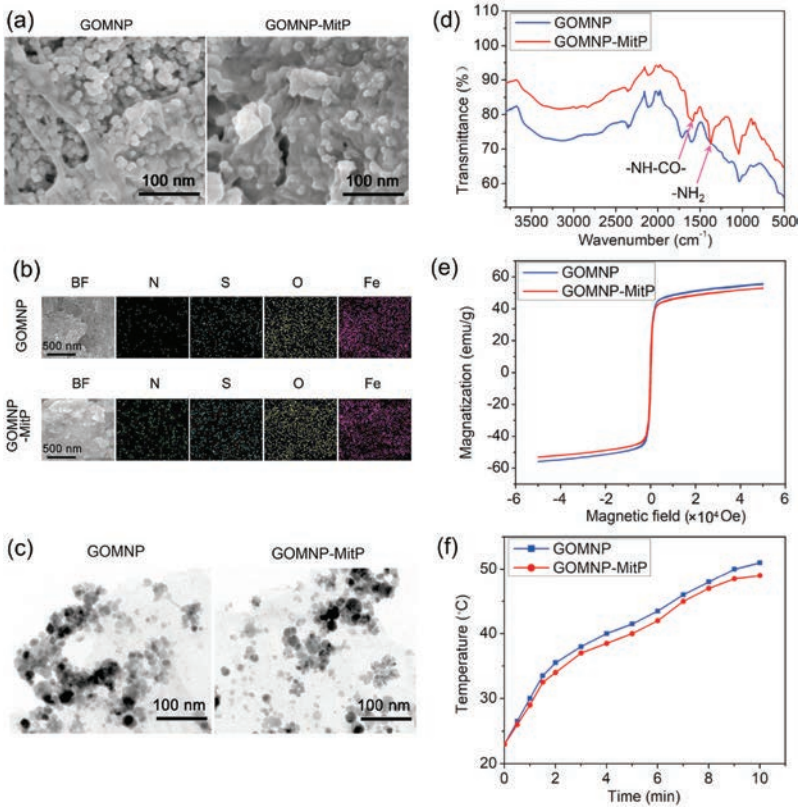

Fig. 1. Characterization of GOMNP and GOMNP-MitP. (a) SEM images. (b) EDS mapping. (c) TEM images. (d) FT-IR spectra. (e) Magnetization curves at 300 K. (f) Temperature curve under AMF treatment.

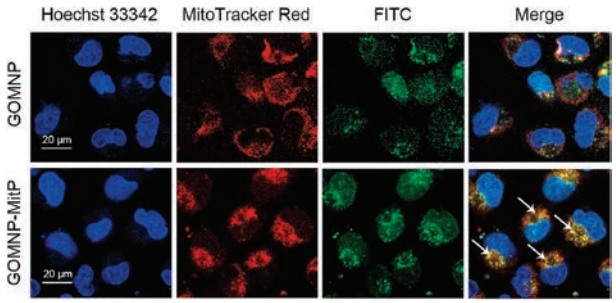

Fig. 3. Mitochondrion-localization of GOMNP-MitP in the A549 tumor cells. The white arrows indicate the representative mitochondrion-localized GOMNP-MitP.

AMF is an important stimulus leading to drug release from magnetic nanocarriers [27,28]. While both GOMNP-MitP and GOMNP did not obviously release MTX in the absence of AMF, both kinds of GOs rapidly released MTX in 30 min and then the release slowly reached to stability (Fig. 2b). Interestingly, GOMNP-MitP released higher percent of MTX than GOMNP (34% *versus* 21% at 30 min, and 38% *versus* 25% at 60 min, Fig. 2b). Therefore, MitP grafting also enhanced the MTX-releasing capacity under AMF stimulus, which may be related to higher MTX levels in GOMNP-MitP than in GOMNP.

Due to the presence of MitP on the surface of GOMNP-MitP, we hypothesized that it might target the mitochondria. Localization of the nanosheets was observed by confocal microscopy. It is worth noting that the FITC-tagged GOMNP nanosheets had random intracellular distribution and did not co-localize with the mitochondria (Fig. 3, top). In contrast, GOMNP-MitP preferentially distributed at the mitochondria in the tumor cells (Fig. 3, down). This result revealed that grafting of MitP rendered the GO nanosheets specifically targeting the mitochondria.

Owing to the mitochondrion-targeting capacity of GOMNP-MitP, the nanosheets might deliver MTX to the mitochondria for further impairing this organelle. The effect of the MTX-loading nanosheets on mitochondrial function-related indicators, including intracellular ATP levels and mitochondrial membrane potential (MMP), was evaluated. Under no AMF treatment, both the MTX-loading GOs and free MTX only led to slight decrease in intracellular ATP levels (Fig. 4a). However, under the AMF treatment, the MTX-loading GOMNP-MitP showed much more severe impact on ATP levels as compared to MTX-loading GOMNP or free MTX (Fig. 4a). Similarly, MMP assays revealed that the MTX-loading GOMNP-MitP led to the most severe reduction of MMP under AMF treatment (Fig. 4b), indicating that the mitochondrial functions were severely impaired by MTX-loading GOMNP-MitP with the aid of AMF.

Mitochondrial damage may lead to release of mitochondrial cytochrome C (Cyt C) to the cytosol, followed by activation of caspase-3 and apoptosis [29,30]. Western blotting assays revealed that MTX-loading GOMNP-MitP with the aid of AMF led to the highest Cyt C release from the mitochondria to the cytosol and up-regulation of activated caspase-3 levels (Figs. 4c and d). These results indicated that the MTX-loading GOMNP-MitP caused most severe mitochondrial damage and further activation of the apoptotic pathway under AMF treatment.

Mitochondrial damage is frequently associated with impairment of cell viability and apoptosis-related cell death [31,32]. As expected, while MTX-loading GOMNP and free MTX only led to slight decrease in cell viability and increase in apoptotic cells, MTX-loading GOMNP rendered drastic decrease in cell viability to < 20%, and remarkable increase in apoptotic cells (> 80%) (Figs. 4e and f) under AMF treatment. Moreover, under the same MTX concentrations (5.5 mg/L), GOMNP-MitP + MTX also had higher impact on cell viability than GOMNP + MTX and MTX (Fig. S1 in Supporting information), indicating that both the enhancement of drug release and the synergism between GOMNP-MitP and MTX contributed to the high anti-tumor capacity of GOMNP-MitP + MTX. Together, these results revealed that the MTX-loading GOMNP with AMF had the highest capacity of impairing the mitochondrial functions and killing the tumor cells.

In conclusion, we designed a kind of two-dimensional magnetic nanoplatform composed of GO, magnetic nanoparticles and MitP, which served as efficient mitochondrion-targeting nanocarriers of anticancer drugs. The anticancer drug-loading nanocarrier GOMNP-MitP could efficiently target the tumor mitochondria and severely disrupt mitochondrial functions for killing the tumor cells with the aid of AMF. This study provides a promising mitochondrion-targeting two-dimensional nanocarrier for efficient anticancer therapy.

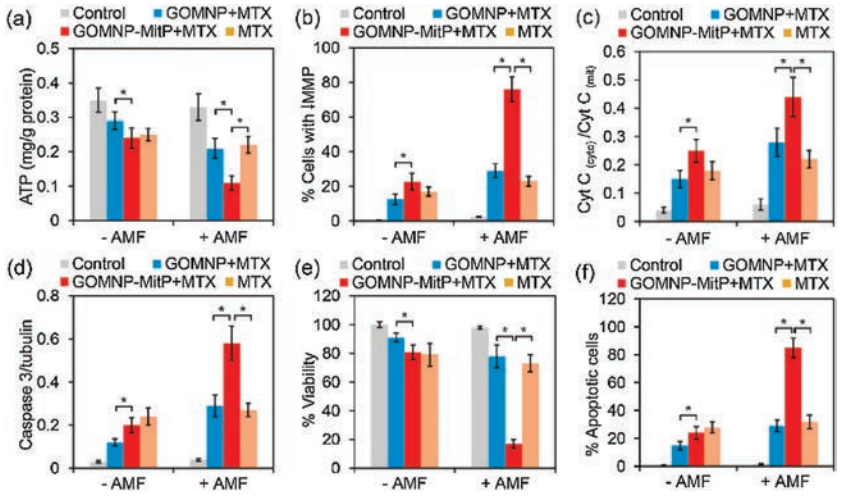

Fig. 4. Impairment of mitochondrial functions and viability by MTX-loading GOMNP-MitP in the A549 tumor cells in the absence of AMF (− AMF) or in the presence of AMF (+ AMF, 375 kHz, 5 kW, 30 min). (a) Intracellular ATP levels. (b) Decrease in MMP. (c) Ratio of cytosol Cyt C (Cyt C $_{(cyto)}$) to mitochondrial Cyt C (Cyt C $_{(mit)}$). (d) Ratio of activated caspase 3 to tubulin. (e) Cell viability revealed by MTT assays. (f) Percent of apoptosis. *indicates significant difference between the groups ($P < 0.05$).

Declaration of competing interest

The authors declare that they have no known competing financial interests or personal relationships that could have appeared to influence the work reported in this paper.

Acknowledgments

This work was supported by National Natural Science Foundation of China (No. 31870139), Natural Science Foundation of Tianjin (No. 19JCZDJC33800), Tianjin Synthetic Biotechnology Innovation Capacity Improvement Project (No. TSBICIP-KJGG-006), and the Fundamental Research for the Central Universities.

Appendix A. Supplementary data

Supplementary material related to this article can be found, in the online version, at doi:https://doi.org/10.1016/j.cclet.2020.09.003.

References

[1] V. Eisner, M. Picard, G. Hajnóczky, Nat. Cell Biol. 20 (2018) 755–765.
[2] E.L. Mills, B. Kelly, L.A.J. O'Neill, Nat. Immunol. 18 (2017) 488–498.
[3] G. Cannino, F. Ciscato, I. Masgras, C. Sánchez-Martín, A. Rasola, Front. Oncol. 8 (2018) 333.
[4] S. Vyas, E. Zaganjor, M.C. Haigis, Cell 166 (2016) 555–566.
[5] S. Jayakumar, R.S. Patwardhan, D. Pal, et al., Free Radic. Biol. Med. 113 (2017) 530–538.
[6] L. Dong, J. Neuzil, Cancer Commun. 39 (2019) 63.
[7] W. Lv, Z. Zhang, K.Y. Zhang, et al., Angew. Chem. Int. Ed. 55 (2016) 9947–9951.
[8] R.X. Zhang, L.Y. Li, J. Li, et al., Adv. Funct. Mater. 27 (2017) 1700804.
[9] L. Yang, P. Gao, Y. Huang, et al., Chin. Chem. Lett. 30 (2019) 1293–1296.
[10] K. Han, J.Y. Zhu, H.Z. Jia, et al., ACS Appl. Mater. Interfaces 8 (2016) 25060–25068.
[11] M. Liu, Y. Lu, Q. Yu, et al., Nano Res. 13 (2020) 1133–1140.
[12] W. Chen, P. Yi, Y. Zhang, et al., ACS Appl. Mater. Interfaces 3 (2011) 4085–4091.
[13] Z. Chen, C. Wu, Z. Zhang, et al., Chin. Chem. Lett. 29 (2018) 1601–1608.
[14] Z. Shi, Q. Li, L. Mei, Chin. Chem. Lett. 31 (2020) 1345–1356.
[15] Y. Chen, P. Xu, Z. Shu, et al., Adv. Funct. Mater. 24 (2014) 4386–4396.
[16] G. Gonçalves, M. Vila, M.T. Portolés, et al., Adv. Healthc. Mater. 2 (2013) 1072–1090.
[17] X. Ma, H. Tao, K. Yang, et al., Nano Res. 5 (2012) 199–212.
[18] Y.S. Huang, Y.J. Lu, J.P. Chen, J. Magn. Magn. Mater. 427 (2017) 34–40.
[19] S.A. Makharza, G. Cirillo, O. Vittorio, et al., Pharmaceuticals 12 (2019) 76.
[20] M.S. Amini-Fazl, R. Mohammadi, K. Kheiri, Int. J. Biol. Macromol. 132 (2019) 506–513.
[21] A.A. Ghawanmeh, G.A. Ali, H. Algarni, S.M. Sarkar, K.F. Chong, Nano Res. 12 (2019) 973–990.
[22] L. Cao, Y. Jiang, Z. Chen, J. Nanosci, Nanotechnol. 18 (2018) 3067–3076.
[23] A. Koceva-Chyła, M. Jedrzejczak, J. Skierski, K. Kania, Z. Jóźwiak, Apoptosis 10 (2005) 1497–1514.
[24] J. Chen, B. Yao, C. Li, G. Shi, Carbon 64 (2013) 225–229.
[25] W.S. Hummers Jr, R.E. Offeman, J. Am. Chem. Soc. 80 (1958) 1339-1339.
[26] Q. Yu, Y.M. Zhang, Y.H. Liu, X. Xu, Y. Liu, Sci. Adv. 4 (2018) eaat2297.
[27] Q. Yu, T. Deng, F.C. Lin, B. Zhang, J.I. Zink, ACS Nano 14 (2020) 5926–5937.
[28] Y. Song, D. Li, Y. Lu, et al., Nat. Sci. Rev. 7 (2020) 723–736.
[29] J.C. Goldstein, N.J. Waterhouse, P. Juin, G.I. Evan, D.R. Green, Nat. Cell Biol. 2 (2000) 156–162.
[30] S. Márquez-Jurado, J. Díaz-Colunga, R.P. Das Neves, et al., Nat. Commun. 9 (2018) 389.
[31] G. Kroemer, J.C. Reed, Nat. Med. 6 (2000) 513–519.
[32] W. Chen, K. Shi, B. Chu, X. Wei, Z. Qian, Nano Lett. 19 (2019) 2905–2913.